Molecules and Cells

K-Ras–Activated Cells Can Develop into Lung Tumors When *Runx3*-Mediated Tumor Suppressor Pathways Are Abrogated

You-Soub Lee[1,3], Ja-Yeol Lee[1,3], Soo-Hyun Song[1], Da-Mi Kim[1], Jung-Won Lee[1], Xin-Zi Chi[1], Yoshiaki Ito[2], and Suk-Chul Bae[1,*]

[1]Department of Biochemistry, School of Medicine, Institute for Tumor Research, Chungbuk National University, Cheongju 28644, Korea, [2]Cancer Science Institute of Singapore, National University of Singapore, Singapore 117599, [3]These authors contributed equally to this work.
*Correspondence: scbae@chungbuk.ac.kr
https://doi.org/10.14348/molcells.2020.0182
www.molcells.org

***K-RAS* is frequently mutated in human lung adenocarcinomas (ADCs), and the p53 pathway plays a central role in cellular defense against oncogenic *K-RAS* mutation. However, in mouse lung cancer models, oncogenic *K-Ras* mutation alone can induce ADCs without p53 mutation, and loss of *p53* does not have a significant impact on early *K-Ras*–induced lung tumorigenesis. These results raise the question of how *K-Ras*–activated cells evade oncogene surveillance mechanisms and develop into lung ADCs. RUNX3 plays a key role at the restriction (R)-point, which governs multiple tumor suppressor pathways including the $p14^{ARF}$–p53 pathway. In this study, we found that *K-Ras* activation in a very limited number of cells, alone or in combination with *p53* inactivation, failed to induce any pathologic lesions for up to 1 year. By contrast, when *Runx3* was inactivated and *K-Ras* was activated by the same targeting method, lung ADCs and other tumors were rapidly induced. In a urethane-induced mouse lung tumor model that recapitulates the features of *K-RAS*–driven human lung tumors, *Runx3* was inactivated in both adenomas (ADs) and ADCs, whereas *K-Ras* was activated only in ADCs. Together, these results demonstrate that the R-point–associated oncogene surveillance mechanism is abrogated by *Runx3* inactivation in AD cells and these cells cannot defend against *K-Ras* activation, resulting in the transition from AD to ADC. Therefore, *K-Ras*–activated lung epithelial cells do not evade oncogene surveillance mechanisms; instead, they are selected if they occur in AD cells in which *Runx3* has been inactivated.**

Keywords: cancer initiation, *K-Ras*, lung cancer, *p53*, *Runx3*

INTRODUCTION

Lung adenocarcinoma (ADC) is the most frequent subtype of lung cancer. Most lung ADCs develop through stepwise progression from atypical adenomatous hyperplasia (AAH) to bronchio-alveolar carcinoma (BAC), and ultimately to multiple types of invasive ADCs (Subramanian and Govindan, 2008; Wistuba and Gazdar, 2006). Human AAH and BAC are considered to be equivalent to mouse lung adenoma (AD). Approximately 25% of human lung ADC cases harbor activating mutations in the *K-RAS* gene. Although K-RAS signaling has been intensely studied, no drugs have yet been approved to treat *K-RAS*–mutant cancers; this is primarily because inhibition of K-RAS, which is important for normal cellular function, would be extremely toxic to patients (Drosten et al., 2018). Therefore, identification of effective tumor

Received 8 September, 2020; accepted 10 September, 2020; published online 26 October, 2020

eISSN: 0219-1032

suppressors of *K-RAS*–dependent lung cancer would provide new strategies for cancer treatment.

RUNX3 is inactivated by epigenetic alterations in most cases of human lung ADs (AAH and BAC) (Lee et al., 2010; 2013) and *K-RAS*–activated lung ADCs (Lee et al., 2013). *Runx3*$^{+/-}$ mice spontaneously develop a variety of tumors in old age, most frequently lung ADs (Lee et al., 2010), and disruption of *Runx3* in mouse lung leads to AD formation (Lee et al., 2013). The cellular decision regarding whether to undergo proliferation or death is made at the restriction (R)-point, which is disrupted in nearly all tumors (Weinberg, 2014). RUNX3 plays a key role at the R-point which governs the p14^{ARF}–p53 pathway (Chi et al., 2017; Lee and Bae, 2020; Lee et al., 2019a; 2019b). Early after mitogenic stimulation, RUNX3 transactivates R-point–associated genes, which include p14^{ARF} (p19^{ARF} in mouse, hereafter ARF) by recruiting activator complexes to its target loci. When the RAS-MEK pathway is downregulated, RUNX3 suppresses the target genes by recruiting repressor complexes. The cell then passes through the R-point to S phase. If the RAS-MEK pathway is not downregulated, expression of the R-point–associated genes are maintained and the cell cannot pass through the R-point. Therefore, the RUNX3 → R-point → ARF → p53 pathway constitutes a surveillance mechanism against oncogenic RAS (Lee et al., 2019a). Indeed, inactivation of *p53* or *Runx3* similarly accelerates malignant progression of oncogenic *K-Ras*–dependent mouse lung tumors (DuPage et al., 2009; Lee et al., 2013).

However, in mouse lung tumor models, oncogenic *K-Ras* mutation alone can induce ADCs without p53 mutation, and loss of *p53* does not have a significant impact on early *K-Ras*–induced lung tumorigenesis (Feldser et al., 2010; Junttila et al., 2010; Muzumdar et al., 2016). Therefore, it remains unclear how *K-Ras*–activated cells evade oncogene surveillance mechanisms. In this study, we analyzed genetically engineered and carcinogen-induced mouse models, and obtained evidence demonstrating that *K-Ras*–activated cells are selected only if the activating *K-Ras* mutation arises in AD cells in which *Runx3* is inactivated.

MATERIALS AND METHODS

Experimental model and subject details

Mice

Runx3^{flox} (Jax 008773), *p53*^{flox} (Jax 008462), *K-Ras*$^{LSL-G12D}$ (Jax 008179), *Rosa26R-Tomato* (Jax 007914), *Cre*$^{tm/ERT1}$ (Jax 004682), and *Cre*$^{tm/ERT2}$ (Jax 008463) mice were obtained from Jackson Laboratory (USA). Unless stated otherwise, all mice analyzed had mixed genetic backgrounds and were age-matched (6-8 weeks old). Sample size was determined based on our experience and previous experiments. No data were excluded from the analysis. Animal experiments described were performed with at least three independent replicates, and representative results are shown in the figures. All animal studies were randomized into control or treated groups; in general, all animals housed in the same cage were in the same treatment group. For analysis of tumor samples, identities were blinded from histopathological assessment. All animals were housed in specific pathogen-free facilities and monitored daily. Animal studies were approved by the Institutional Animal Care Committee of Chungbuk National University (CBNUA-1208-18-02).

Method details

Adenovirus delivery

Adenovirus carrying Cre recombinase (*Ad-Cre*) was purchased from Vector Biolabs (USA). Each mouse was treated with 2.5×10^7 *Ad-cre* viral genome copies diluted in warm 50 μl sterile MEM. After treatment, mice were placed on a warm pad until they woke up .

Chemical delivery

To determine the order of *Runx3* inactivation and *K-Ras* activation during urethane-induced development of lung ADC, 6-week-old wild-type (WT) mice were injected intraperitoneally with urethane (ethylcarbamate; Sigma, USA) (500 mg/kg body weight).

Hematoxylin and eosin staining

H&E staining was conducted according to a standard protocol. Briefly, slides were rehydrated by ethanol, xylene, and water to remove the paraffin. The nuclei were stained with hematoxylin (#S3309; DAKO, USA) for 3 min, and the cytoplasm was stained with eosin (HT110280; Sigma) for 30 s. Slides were mounted with Permount (SP15-500; Thermo Fisher Scientific, USA) after the dehydration and clearing steps.

Histology and immunohistochemistry

For histological analysis, lungs were inflated with 4% paraformaldehyde or formalin (3.7% formaldehyde) and fixed for 36 h. Fixed paraffin sections were rehydrated, subjected to antigen retrieval, and blocked in Tris-buffered saline (0.1% Triton X-100 containing 1% bovine serum albumin) or protein-free blocking solution (DAKO), and sequentially incubated with specific primary antibodies and biotinylated (DAKO) or Alexa Fluor-conjugated secondary antibodies (Invitrogen, USA). Images were produced with a conventional microscope mounted with a DP71 digital camera (Olympus, Japan), an LSM 710 T-PMT confocal microscope (Carl Zeiss, Germany), and an AXIO Zoom.V16 and ApoTome.2 (Carl Zeiss). Images were processed with equivalent parameters using the ZEN Light Edition software (Carl Zeiss).

DNA exon-sequencing analysis

Standard exome-capture libraries were generated from 1 μg input DNA using the Agilent SureSelect Target Enrichment protocol for Illumina paired-end sequencing library (ver. B.3, June 2015). Probe sets were SureSelect Human All-Exon V6 or SureSelect Mouse All-Exon (Agilent, USA). DNA was quantitated using PicoGreen, and DNA quality was assessed by agarose gel electrophoresis. One microgram of DNA from each cell line was diluted in EB buffer and sheared to a target peak size of 150 to 200 bp using the Covaris LE220 focused ultrasonicator (Covaris, USA). The 8-microTUBE Strips were loaded into the tube holder of the ultrasonicator, and the

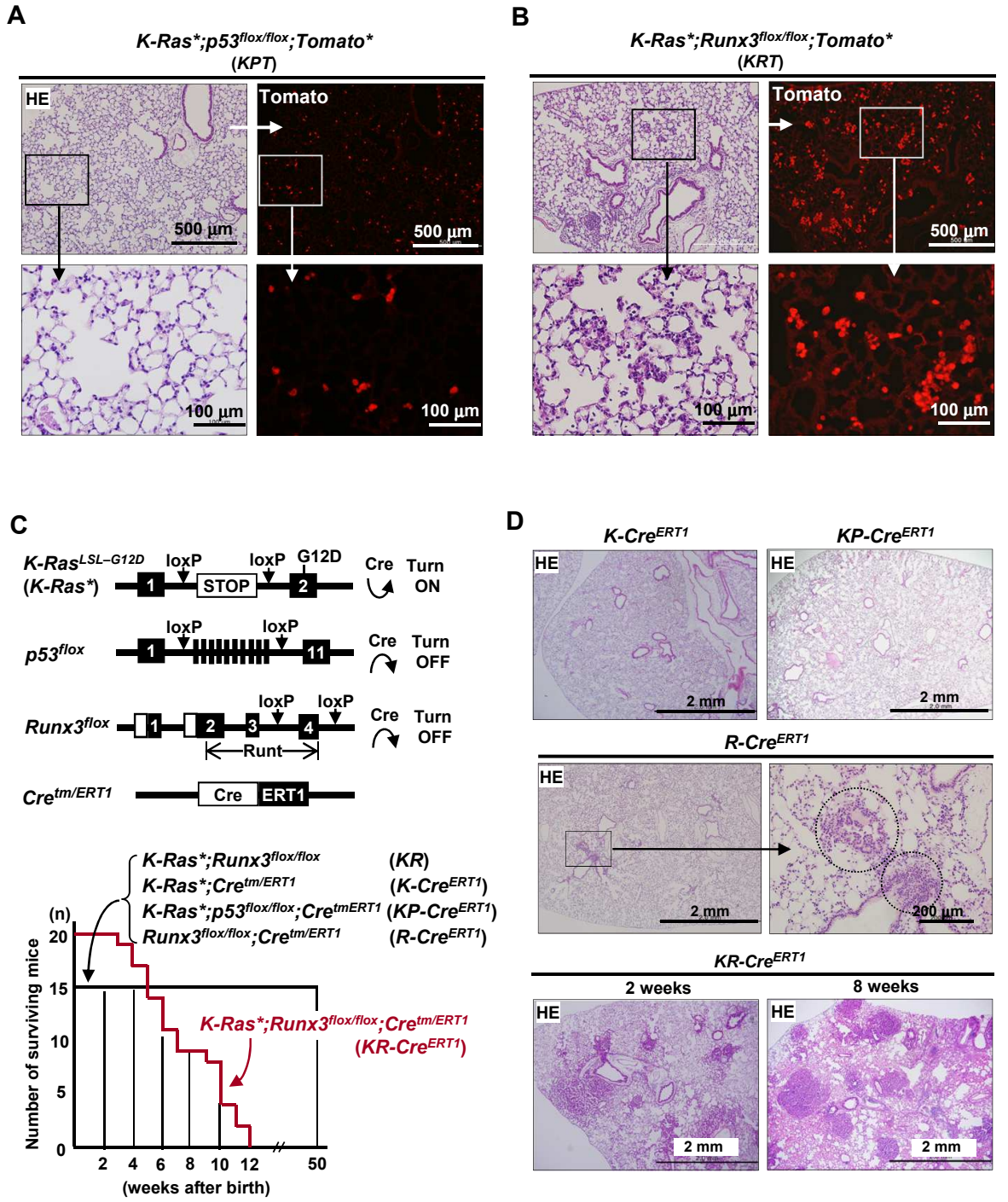

Fig. 1. *Runx3* inactivation, but not *p53* inactivation, enables immediate proliferation of *K-Ras*-activated lung epithelial cells. (A and B) *KPT* and *KRT* mice were targeted with *Ad-Cre* (2.5×10^7 PFU/mouse, as described by DuPage et al., 2009), and Tomato-positive lung epithelial cells were assessed after 10 days. Clusters of Tomato-positive cells were detected 10 days after infection only in *KRT* mice lungs. Enlarged images of the boxed regions are shown (lower panels). (C) Schematic representation of the structures of *K-Ras*$^{LoxP\text{-}STOP\text{-}LoxP\text{-}G12D}$ (*K-Ras**), *Runx3*^{flox}, *p53*^{flox}, and *Cre*$^{tm/ERT1}$ (*Cre*^{ERT1}) alleles. Cre recombinase activates *K-Ras* by removal of a knocked-in STOP transcriptional cassette from the *K-Ras*$^{LoxP\text{-}STOP\text{-}LoxP\text{-}G12D}$ allele and inactivates the *p53*^{flox} and *Runx3*^{flox} alleles by deletion of exons. Survival curves of *KR*, *R-Cre*^{ERT1}, *K-Cre*^{ERT1}, *KP-Cre*^{ERT1}, and *KR-Cre*^{ERT1} mice in the absence of tamoxifen are shown. The median survival of *KR-Cre*^{ERT1} mice was 48 days. No mice of other genotypes died within 50 weeks after birth (the duration of the experiment). (D) Hematoxylin/eosin (HE) staining of the lungs of *K-Cre*^{ERT1}, *KP-Cre*^{ERT1}, and *R-Cre*^{ERT1} mice (6 months after birth). A magnified image of the boxed region is shown on the right. Adenomatous lesions in a *R-Cre*^{ERT1} lung are indicated by dotted circles. HE staining of the lung tumors of *KR-Cre*^{ERT1} mice (2 and 8 weeks after birth).

DNA was sheared using the following settings: mode, frequency sweeping; duty cycle, 10%; intensity, 5; cycles per burst, 200; duration, 60 s × 6 cycles; temperature, 4°C to 7°C. The fragmented DNA was repaired, an 'A' was ligated to the 3′ end, and Agilent adapters were ligated to the fragments. Once ligation was assessed, the adapter ligated product was amplified by polymerase chain reaction (PCR). The final purified product was quantified using TapeStation DNA ScreenTape D1000 (Agilent). For exome capture, 250 ng of DNA library was mixed with hybridization buffers, blocking mixes, RNase block, and 5 μl of SureSelect All-Exon capture library according to the standard Agilent SureSelect Target Enrichment protocol. Hybridization to the capture baits was conducted for 24 h at 65°C in a PCR machine, with the thermal cycler lid heated to 105°C. The captured DNA was washed and amplified. The final purified product was quantified by qPCR according to the qPCR Quantification Protocol Guide (KAPA Library Quantification kits for Illumina Sequencing platforms) and quantified again using the TapeStation DNA ScreenTape D1000 (Agilent). Finally, the DNA was sequenced on the HiSeq 2500 platform (Illumina, USA).

RESULTS

Runx3 inactivation, but not *p53* inactivation, enables immediate proliferation of *K-Ras*-activated lung epithelial cells

To determine whether the oncogenic *K-RAS* → RUNX3 → ARF → p53 pathway suppresses proliferation of *K-Ras*-activated lung epithelial cells *in vivo*, we crossed *Rosa26R-Tomato* (*Tomato**) mice with strains harboring *Runx3*$^{flox/flox}$, *p53*$^{flox/flox}$, and *K-Ras*$^{LoxP\text{-}STOP\text{-}LoxP\text{-}G12D/+}$ (*K-Ras**), yielding *K-Ras*;p53*$^{flox/flox}$*;Tomato** (*KPT*) and *K-Ras*;Runx3*$^{flox/flox}$*;Tomato** (*KRT*) mice. The mice were targeted by *Cre*-expressing adenovirus infection (*Ad-Cre*, 2.5×10^7 pfu/mouse; DuPage et al., 2009), and the Tomato-positive cells were traced 10 days after infection. The results revealed that most of the *p53*-inactivated and *K-Ras*–activated cells remained as single cells, i.e., they had not divided (Fig. 1A). By contrast, most of the *Runx3*-inactivated and *K-Ras*–activated cells had formed clusters (Fig. 1B). These results indicate that *Runx3* inactivation, but not *p53* inactivation, enables immediate proliferation of *K-Ras*–activated lung epithelial cells.

Runx3 inactivation allows initiation of *K-Ras*-dependent lung cancer

Currently, all available genetically engineered *K-Ras*–dependent mouse lung cancer models require activation of *K-Ras* in a large number of cells (10^6-10^8 cells/mouse) and a long latency period (Guerra et al., 2003; Tuveson et al., 2004). Under physiological conditions, however, activation of *K-Ras* does not occur simultaneously in a large number of cells. Therefore, we asked whether activation of *K-Ras*, alone or in combination with inactivation of *p53* or *Runx3*, in a very small number of cells could induce lung cancer. To target *Runx3*, *p53*, and/or *K-Ras* in a very small number of cells, we crossed *Cre*$^{tm/ERT1}$ mice with strains harboring *Runx3*$^{flox/flox}$, *p53*$^{flox/flox}$, and *K-Ras** and obtained various genotype combinations. In these mice, Cre recombinase can be activated with tamoxifen to activate *K-Ras* and inactivate *p53* or *Runx3* (Fig. 1C). However, due to weak Cre leakage in this model, in the absence of tamoxifen, genes are targeted in very few cells (Kemp et al., 2004), providing a convenient means of targeting a limited number of cells. Therefore, we examined tumor formation and survival in these mice in the absence of tamoxifen.

All *K-Ras*;Runx3*$^{flox/flox}$ (*KR*), *K-Ras*;Cre*$^{tm/ERT1}$ (*K-Cre*^{ERT1}), *K-Ras*;p53*$^{flox/flox}$*;Cre*$^{tm/ERT1}$ (*KP-Cre*^{ERT1}), and *Runx3*$^{flox/flox}$*;Cre*$^{tm/ERT1}$ (*R-Cre*^{ERT1}) mice survived for more than 1 year (Fig. 1C). Pathological analysis revealed that the mice were completely tumor-free (Fig. 1D), whereas *R-Cre*^{ERT1} mice developed a few small ADs (Fig. 1D). By contrast, all mice with the *K-Ras*;Runx3*$^{flox/flox}$*;Cre*$^{tm/ERT1}$ (*KR-Cre*^{ERT1}) genotype developed lung ADCs rapidly, as early as 2 weeks after birth, and died within 12 weeks of birth in the absence of tamoxifen (median survival, 48 days) (Figs. 1C and 1D). These results indicated that while activation of *K-Ras* alone or in combination with inactivation of *p53* in a small number of cells does not result in lung cancer formation, concurrent *K-Ras* activation and *Runx3* inactivation does.

To determine whether the same thing would happen when *K-Ras* activation and *Runx3* inactivation occurred in an even smaller number of cells, we used Cre$^{tm/ERT2}$, which is much more tightly regulated by tamoxifen than Cre$^{tm/ERT1}$. These experiments were performed in *Rosa26R-Tomato* (*Tomato**) mice to allow visualization of the targeted cells. *Cre*$^{tm/ERT2}$ mice and *Tomato** mice were crossed with *Runx3*$^{flox/flox}$, *p53*$^{flox/flox}$, and *K-Ras** mice to obtain *Tomato*;Cre*$^{tm/ERT2}$ (*T-Cre*^{ERT2}), *K-Ras*;Tomato*;Cre*$^{tm/ERT2}$ (*KT-Cre*^{ERT2}), *K-Ras*;p53*$^{flox/flox}$*;Tomato*; Cre*$^{tm/ERT2}$ (*KPT-Cre*^{ERT2}), and *K-Ras*; Runx3*$^{flox/flox}$*;Tomato*;Cre*$^{tm/ERT2}$ (*KRT-Cre*^{ERT2}) mice. The mice were maintained in the absence of tamoxifen. Six months after birth, a few Tomato-positive cells (average, 20 cells per section) were detected in the lungs of *T-Cre*^{ERT2} mice (Fig. 2A), confirming that Cre$^{tm/ERT2}$, like Cre$^{tm/ERT1}$, is leaky. However, Tomato-positive cells in the lungs of *KT-Cre*^{ERT2} mice were extremely rare (average, 0.5 cells per section) (Fig. 2A). Simple calculation suggests that only about 2.5% of *K-Ras*–activated cells survived, and that these cells were in a quiescent state. These results suggest that the majority of *K-Ras*–alone-activated cells are eliminated through oncogene surveillance mechanisms.

Similar to what we observed with *Cre*$^{tm/ERT1}$ mice, *KPT-Cre*^{ERT2} mice (n = 5) were completely tumor-free 6 months after birth (Fig. 2B). By contrast, all *KRT-Cre*^{ERT2} mice (n = 5) developed lung ADCs (Fig. 2B). In the lungs of *KPT-Cre*^{ERT2} mice, we detected clusters of Tomato-positive cells, but these cells formed a normal alveolar architecture and did not exhibit any dysplastic features (Fig. 2C). These results suggest that *p53* inactivation enables *K-Ras*–activated cells to survive and weakly proliferate, but not to develop into tumors. By contrast, Tomato-positive cells in *KRT-Cre*^{ERT2} mouse lungs formed tumors (Fig. 2D), indicating that *Runx3* inactivation enables *K-Ras*–activated cells not only to survive and proliferate, but also to develop into tumors. These results suggest that *p53* inactivation abrogates the oncogene surveillance mechanism only partly, whereas *Runx3* inactivation does so completely.

Overall, these findings indicate that *K-Ras* activation in a

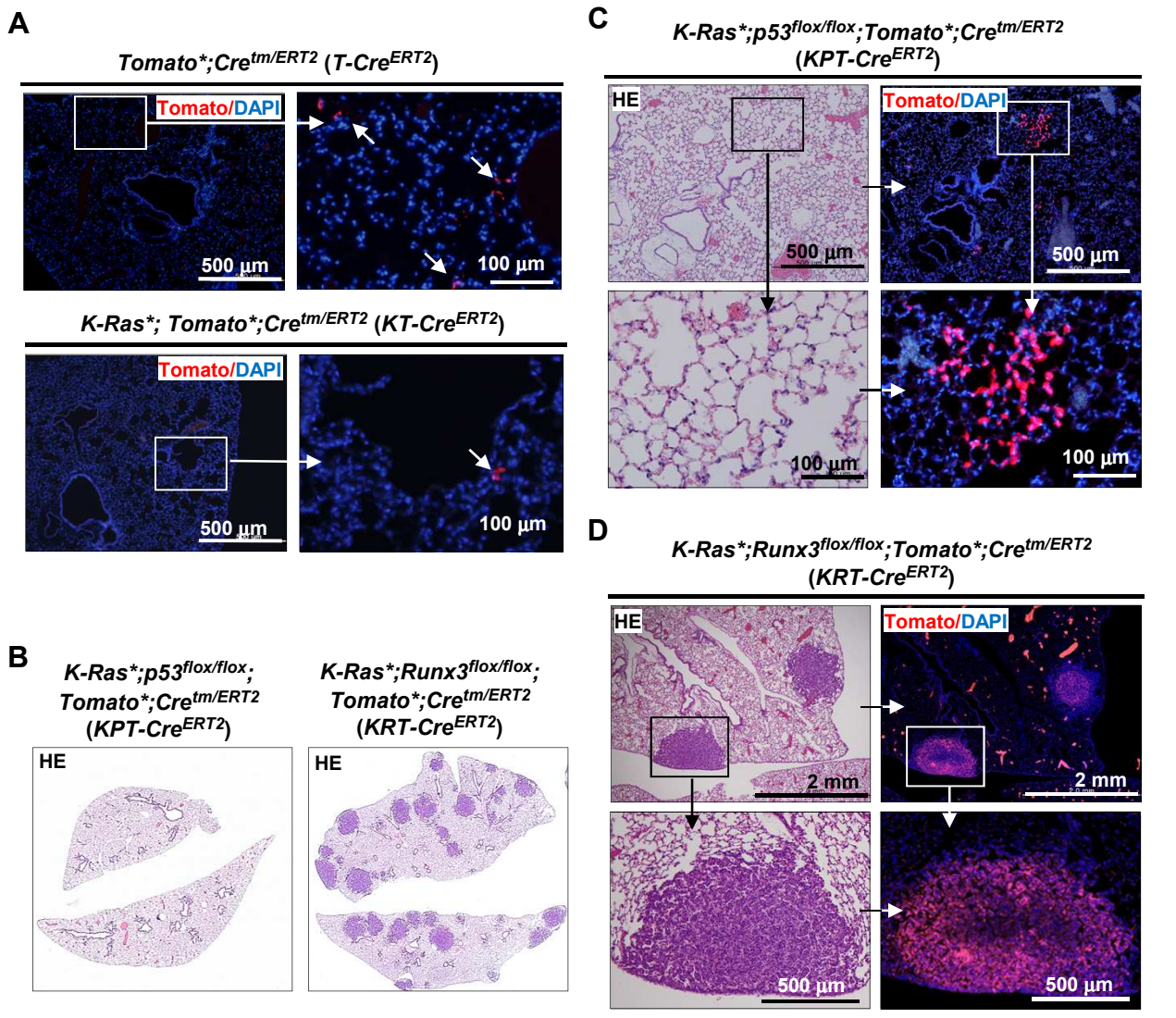

Fig. 2. The combination of *K-Ras* activation and *Runx3* inactivation is the minimum molecular requirement for induction of lung tumor formation. (A) Microscopic images of lungs of *T-Cre*^{ERT2} and *KT-Cre*^{ERT2} mouse (6 months after birth) stained with anti-Tomato antibody. Tomato-positive cells (red) are indicated by arrows. (B) HE staining of the lungs of *KPT-Cre*^{ERT2} and *KRT-Cre*^{ERT2} mice (6 months after birth). (C and D) Microscopic images of lungs of *KPT-Cre*^{ERT2} mice and *KRT-Cre*^{ERT2} mice (6 months after birth) stained with HE or anti-Tomato antibody. Magnified images of the boxed regions are shown (lower panels). Small clusters of Tomato-positive cells were detected in *KPT-Cre*^{ERT2} mice, but did not develop into cancers. By contrast, Tomato-positive cells in *KRT-Cre*^{ERT2} mice developed into cancers.

limited number of cells, either alone or in combination with *p53* inactivation, does not induce lung cancer, whereas the combination of *K-Ras* activation and *Runx3* inactivation immediately induces lung cancer. These results suggest that *Runx3* functions as a gatekeeper against *K-Ras*–dependent lung tumorigenesis.

The gatekeeper activity of *Runx3* against *K-Ras* activation also operates in other tissues

Leaky activation of Cre$^{tm/ERT1}$ occurs in a wide range of tissues (Kemp et al., 2004). Indeed, tumors in *KR-Cre*^{ERT1} mice were not limited to the lungs. Although lung ADCs developed in all *KR-Cre*^{ERT1} mice, other types of tumors also developed. In particular, six of twenty *KR-Cre*^{ERT1} mice developed skin cancers in the anus (Fig. 3A), six had a grossly enlarged spleen with massive lymphoid hyperplasia (Fig. 3B), and seven had an enlarged thymus with thymic lymphoma (Fig. 3B). None of these tumors were detected in *KP-Cre*^{ERT1} mice.

Notably, thymic lymphoma cells infiltrated into the lung along the broncho-vascular bundle in some *KRT-Cre*^{ERT2} mice (Fig. 3C). The targeting of *K-Ras** and *Runx3*$^{flox/flox}$ by leaky activation of Cre$^{tm/ERT1}$ or Cre$^{tm/ERT2}$ in the tumors was confirmed by genotyping (Fig. 3D). These results imply that the proposed gatekeeper activity of *Runx3* against *K-Ras* ac-

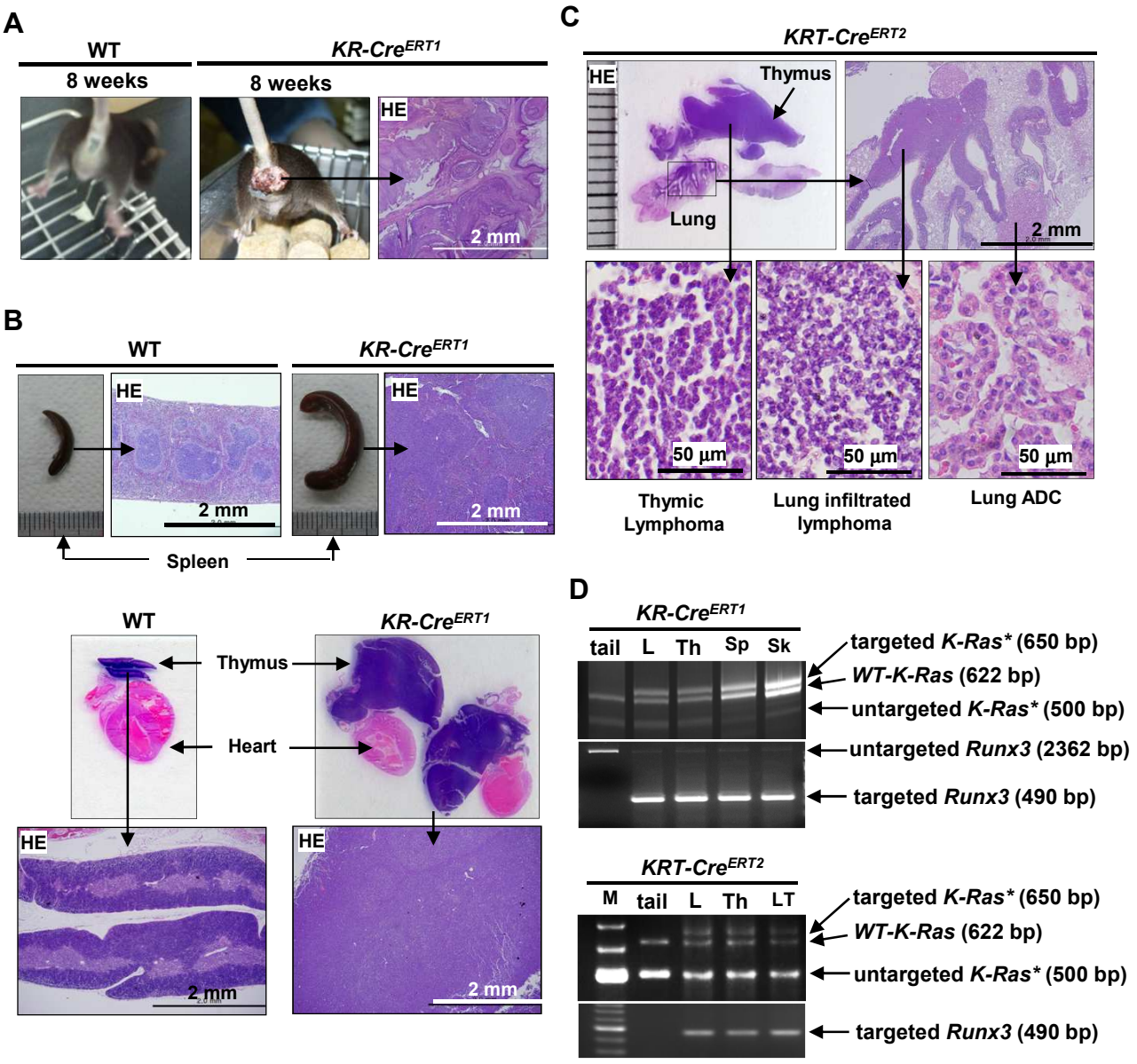

Fig. 3. *KR-Cre*^{ERT1} mice develop lymphomas and skin cancers, as well as lung ADs/ADCs. (A) Gross and microscopic images of a skin cancer that developed in a *KR-Cre*^{ERT1} mouse. (B) Gross and microscopic images of the spleen and thymus of WT and *KR-Cre*^{ERT1} mice. Histological analysis revealed that the cortex-medulla boundary in the enlarged thymuses was obscure and filled with undifferentiated T-cells, indicating thymic lymphoma. (C) HE-stained gross images and magnified microscopic images of thymus and lung of *KRT-Cre*^{ERT2} mice (6 months after birth). Lung-invading tumor cells were morphologically identical to thymic lymphoma cells, indicating that the lung-invading tumors originated from a thymic lymphoma. (D) Targeting of the *K-Ras** and *Runx3*^{flox} alleles by leaky activation of Cre^{ERT1} in tumors was verified by genomic PCR. L, lung ADC; Th, thymus; Sp, spleen; Sk, skin cancer. Targeting of the *K-Ras** and *Runx3*^{flox} alleles by leaky activation of Cre^{ERT2} in tumors was verified by genomic PCR. M, DNA size marker; L, lung ADC; Th, thymus; LT, lung infiltrated thymic lymphoma.

tivation is not limited to the lung, but also operates in other tissues.

Lung ADs develop via inactivation of *Runx3* and progress into ADCs via *K-Ras* activation

Mouse lung tumors induced by urethane, a tobacco carcinogen, recapitulate the natural history of smoking-associated, *K-RAS*–driven human lung ADCs (Westcott et al., 2015). The mice develop slow-growing ADs about 20 weeks after urethane treatment and fast-growing ADCs about 58 weeks later (Fig. 4A). We previously showed that *Runx3* expression is downregulated in nearly all urethane-induced lung ADs and ADCs, mainly due to hypermethylation of the *Runx3* CpG island (Lee et al., 2010). In this study, we detected K-Ras path-

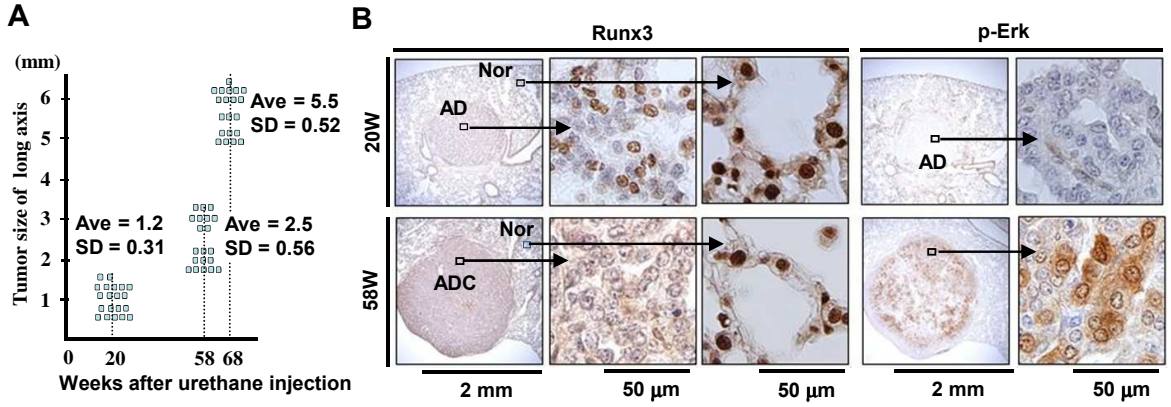

C

Tumors	Size	#1	#2	#3	#4
AD (20W)	d<1 mm	0%	0%	0%	0%
ADC (58W-S)	d≒2 mm	G61R (23%)	G12V (19%)	G61L (23%)	G61R (23%)
ADC (58W-L)	d≒3 mm	G61R (29%)	G61R (34%)	G61A (36%)	G61A (35%)
ADC (68W)	d≒6 mm	G61A (40%)	G61A (41%)	G61A (41%)	G61L (54%)

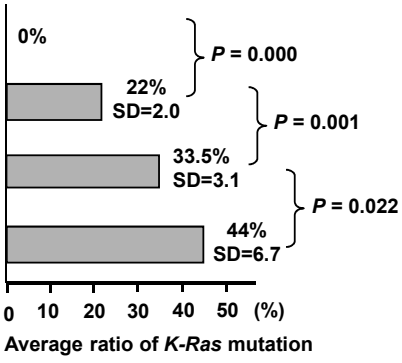

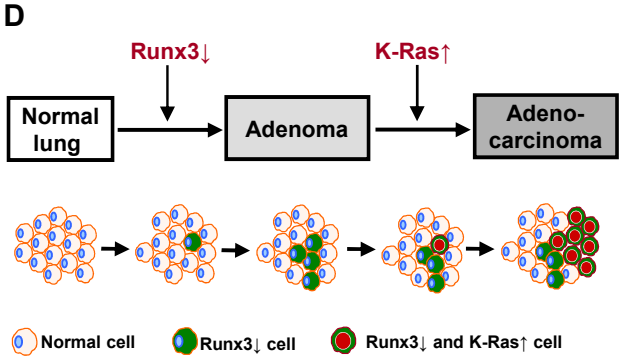

Fig. 4. Sequential molecular events associated with the development of lung AD and progression to ADC. (A) Mice (FVB strain) were intraperitoneally injected with urethane at a dose of 500 mg/kg body weight. Growth of cancer in mouse lungs vs. time after urethane injection is shown. Five mice were used for each time point. Ave, average diameter (mm) of cancer; SD, standard deviation. (B) Mouse lung ADs that developed 20 weeks (20W) after urethane injection and lung ADCs that developed 58 weeks (58W) after injection were analyzed by immunohistochemical (IHC) staining with anti-phospho-Erk (p-Erk) and anti-Runx3 antibodies. *Runx3* expression was markedly downregulated in both ADs and ADCs relative to adjacent normal regions. By contrast, Erk was activated only in ADCs. Nor, normal. (C) WT mouse lung and mouse lung ADs developed at 20 weeks (20W, diameter < 1 mm), relatively small lung ADCs (58W-S, diameter ≒ 2 mm) and relatively large lung ADCs (58W-L, diameter ≒ 3 mm) developed at 58 weeks, and large lung ADCs (68W-L, diameter ≒ 6 mm) developed at 68 weeks after urethane injection were obtained. Four ADs or ADCs from each group were analyzed by whole-exon sequencing. Among the known major oncogenes and tumor suppressors involved in lung cancer, only *K-Ras* mutations were detected. Amino acid changes in K-Ras and the ratio of mutation signal to total signal are shown. d, diameter; ratio, ratio of oncogenic *K-Ras*-mutated allele relative to total *K-Ras*. Bar diagram demonstrating average ratios of *K-Ras* mutation in each group of ADs/ADCs. *P* = *P* value. (D) Schematic representation of the molecular events associated with the development of lung ADs and progression into ADCs. Runx3↓ and K-Ras↑ indicate *Runx3* inactivation and *K-Ras* activation, respectively. Human AAH and BAC correspond to mouse lung ADs.

way activation (Erk phosphorylation) in almost all ADCs (19 out of 20), but not in any ADs (n = 20) in which *Runx3* was inactivated (Fig. 4B). Consistent with this, whole-exon sequencing revealed that oncogenic *K-Ras* mutation was present in all ADCs but in no ADs (Fig. 4C, Supplementary Data 1). No mutations within exons of other known oncogenes and tumor suppressors involved in lung cancer were detected in ADs or ADCs (Supplementary Data 1). Notably, the proportion of oncogenic *K-Ras*–mutated alleles (representing the proportion of *K-Ras*–mutated cells within the tumor) increased with cancer growth (Fig. 4C). These results, together with our previous observations that *Runx3* deletion in mouse lung results in development of AD (Lee et al., 2013), suggest that lung ADs develop via inactivation of *Runx3*, and that AD cells that acquire oncogenic *K-Ras* mutation selectively proliferate and form ADCs (Fig. 4D).

DISCUSSION

Although *K-RAS* mutation is the most frequently detected oncogenic mutation in human cancers, to date no drugs have been approved to treat *K-RAS*–mutant cancers. Recently, oncogenic K-RAS–specific inhibitors have been developed and are currently in clinical trials (Canon et al., 2019). However, more recent reports show that shortly after treatment with these inhibitors, some cancer cells bypass the effect of oncogenic K-RAS inhibition and resume proliferation (Xue et al., 2020). In addition, even when a cancer is effectively regressed by knockdown of oncogenic *K-Ras* in a mouse lung cancer model, the cancer recurs rapidly, not because the gene knockdown was unsuccessful but because other oncogenes were activated (Shao et al., 2014). These results suggest that existing strategies for inhibiting oncogenic K-RAS have a limited ability to achieve a durable response in cancer treatment. Given that normal mice do not suffer from tumors as frequently as tumor-regressed mice, the rapid recurrence phenomenon observed in cancer-regressed mice (Shao et al., 2014) implies that a defense mechanism is abrogated in *K-Ras*–activated lung tumors. However, loss of *p53* does not have a significant impact on early *K-Ras*–induced lung tumorigenesis (Feldser et al., 2010). These observations imply the existence of an effective defense mechanism against oncogenic *K-Ras* signaling, and that this mechanism is disrupted by a hidden molecular event in *K-Ras*–dependent lung cancers. Therefore, to achieve a complete and durable response, it will be necessary to identify the hidden defense mechanism against *K-Ras*–dependent lung cancers.

To confirm the existence of this defense mechanism and identify the critical genes involved, we need to understand why tumor development in animal models requires activation of oncogenes in a large number of cells. For example, *K-Ras*–dependent mouse models develop lung cancer several months after *K-Ras* is targeted in a large number of cells (10^6-10^8 cells/mouse) (Guerra et al., 2003; Tuveson et al., 2004). Therefore, cancer development must be a very rare event within the large population of *K-Ras*–activated cells. To explain this, we can consider two possibilities. First, the cells that originate the tumors may be very rare, making the probability of targeting *K-Ras* in any given origin cell very low (single-step model, assuming the absence of a defense mechanism). Second, the cells of origin of tumors may be relatively abundant, but *K-Ras* activation alone cannot induce cancer unless the defense mechanism is abrogated (two-step model, assuming the existence of the defense mechanism). In this study, we observed the following: (1) A combination of *Runx3* inactivation and *K-Ras* activation in a very limited number of cells immediately induced lung ADCs, whereas *K-Ras* activation alone or in combination with *p53* inactivation did not. (2) In the carcinogen-induced mouse lung cancer model, *Runx3* inactivation occurred earlier than *K-Ras* activation. Our results strongly support the second possibility described above, which assumes the existence of the defense mechanism: the majority of lung ADs are initiated by *Runx3* inactivation, and AD cells, in which R-point-associated oncogene surveillance mechanism is abrogated, cannot defend against *K-Ras* activation, resulting in a transition from ADs to ADC.

The Arf–p53 pathway is the primary defense against oncogenic *Ras* in primary cells (Serrano et al., 1997). Why, then, is only limited tumor suppressor activity of p53 observed in mouse lung tumor models (Feldser et al., 2010)? In our interpretation, the results do not imply a limitation of p53 tumor suppressor activity, but instead suggest that p53-independent tumor suppressive mechanisms exist in the lung; hence, if lung tumorigenesis is suppressed by multiple pathways, loss of p53 can be compensated by other pathways. In this regard, it is worth emphasizing that the R-point, which is disrupted in nearly all tumors, governs multiple tumor suppression pathways (Weinberg, 2014). When a death decision is made at the R-point, the cell defends against tumorigenesis by regulating not only intracellular programs (cell cycle, apoptosis, and metabolism) but also extracellular programs (inflammatory and immune responses) (Lee et al., 2019a; Samarakkody et al., 2020; Seo and Taniuchi, 2020). Because Runx3 functions as a decision-maker of the R-point, inactivation of *Runx3* abrogates the entire R-point–associated defense programs (Lee et al., 2019a). By contrast, p53 functions as an executor of the R-point decision, and inactivation of the gene abrogates only intracellular programs. The critical roles of *Runx3* in R-point regulation may explain how *Runx3* functions as a potent gatekeeper against oncogenic *K-Ras*.

Targeted therapies that inhibit activated oncogenes have yielded clinical responses but eventually lead to cancer recurrence with secondary oncogene activation in almost all malignancies (Janne et al., 2009; Podsypanina et al., 2008). Therefore, it would be of great therapeutic value to understand why cancers recur after the failure of therapies that target activated oncogenes. Our results explain why cancers recur: inhibition of an activated oncogene causes the cancer to regress, but the regressed cells remain cancer-prone because their oncogene surveillance mechanisms are inactivated.

Note: Supplementary information is available on the Molecules and Cells website (www.molcells.org).

ACKNOWLEDGMENTS

S-C Bae is supported by a Creative Research Grant (2014R1A3A2030690) through the National Research Foun-

dation (NRF) of Korea. Y-S Lee is supported by Basic Science Research Program grant 2017R1D1A3B03034076. J-W Lee is supported by Basic Science Research Program grant 2018R1C1B6001532. Y Ito is supported by the Singapore Ministry of Health's National Medical Research Council under its Open Fund Large Collaborative Grant (LCG) Programme (MOH-OFLCG18MAY-0003), NRF Singapore, and the Singapore Ministry of Education under its Research Centres of Excellence initiative.

AUTHOR CONTRIBUTIONS

Y.S.L., J.Y.L., and D.M.K. generated mouse cancer models and analyzed the cancers. X.Z.C. analyzed inactivation, activation, and restoration of target genes in mouse cancer models. J.W.L. and S.H.S. analyzed *K-Ras* mutations in mouse cancers. Y.I. and S.C.B. interpreted the results. S.C.B. planned the experiments and wrote the manuscript. All authors contributed to the editing of the manuscript.

CONFLICT OF INTEREST

The authors have no potential conflicts of interest to disclose.

ORCID

You-Soub Lee	https://orcid.org/0000-0002-2893-4994
Ja-Yeol Lee	https://orcid.org/0000-0002-6064-6271
Soo-Hyun Song	https://orcid.org/0000-0003-4093-023X
Da-Mi Kim	https://orcid.org/0000-0003-2445-8289
Jung-Won Lee	https://orcid.org/0000-0002-5253-3322
Xin-Zi Chi	https://orcid.org/0000-0001-7592-6105
Yoshiaki Ito	https://orcid.org/0000-0002-9037-1184
Suk-Chul Bae	https://orcid.org/0000-0002-4613-3517

REFERENCES

Canon, J., Rex, K., Saiki, A.Y., Mohr, C., Cooke, K., Bagal, D., Gaida, K., Holt, T., Knutson, C.G., Koppada, N., et al. (2019). The clinical KRAS(G12C) inhibitor AMG 510 drives anti-tumour immunity. Nature *575*, 217-223.

Chi, X.Z., Lee, J.W., Lee, Y.S., Park, I.Y., Ito, Y., and Bae, S.C. (2017). Runx3 plays a critical role in restriction-point and defense against cellular transformation. Oncogene *36*, 6884-6894.

Drosten, M., Guerra, C., and Barbacid, M. (2018). Genetically engineered mouse models of K-Ras-driven lung and pancreatic tumors: validation of therapeutic targets. Cold Spring Harb. Perspect. Med. *8*, a031542.

DuPage, M., Dooley, A.L., and Jacks, T. (2009). Conditional mouse lung cancer models using adenoviral or lentiviral delivery of Cre recombinase. Nat. Protoc. *4*, 1064-1072.

Feldser, D.M., Kostova, K.K., Winslow, M.M., Taylor, S.E., Cashman, C., Whittaker, C.A., Sanchez-Rivera, F.J., Resnick, R., Bronson, R., Hemann, M.T., et al. (2010). Stage-specific sensitivity to p53 restoration during lung cancer progression. Nature *468*, 572-575.

Guerra, C., Mijimolle, N., Dhawahir, A., Dubus, P., Barradas, M., Serrano, M., Campuzano, V., and Barbacid, M. (2003). Tumor induction by an endogenous K-ras oncogene is highly dependent on cellular context. Cancer Cell *4*, 111-120.

Janne, P.A., Gray, N., and Settleman, J. (2009). Factors underlying sensitivity of cancers to small-molecule kinase inhibitors. Nat. Rev. Drug Discov. *8*, 709-723.

Junttila, M.R., Karnezis, A.N., Garcia, D., Madriles, F., Kortlever, R.M., Rostker, F., Brown Swigart, L., Pham, D.M., Seo, Y., Evan, G.I., et al. (2010). Selective activation of p53-mediated tumour suppression in high-grade tumours. Nature *468*, 567-571.

Kemp, R., Ireland, H., Clayton, E., Houghton, C., Howard, L., and Winton, D.J. (2004). Elimination of background recombination: somatic induction of Cre by combined transcriptional regulation and hormone binding affinity. Nucleic Acids Res. *32*, e92.

Lee, J.W. and Bae, S.C. (2020). Role of RUNX family members in G_1 restriction point regulation. Mol. Cells *43*, 182-187.

Lee, J.W., Kim, D.M., Jang, J.W., Park, T.G., Song, S.H., Lee, Y.S., Chi, X.Z., Park, I.Y., Hyun, J.W., Ito, Y., et al. (2019a). RUNX3 regulates cell cycle-dependent chromatin dynamics by functioning as a pioneer factor of the restriction-point. Nat. Commun. *10*, 1897.

Lee, J.W., Park, T.G., and Bae, S.C. (2019b). Involvement of RUNX and BRD family members in restriction point. Mol. Cells *42*, 836-839.

Lee, K.S., Lee, Y.S., Lee, J.M., Ito, K., Cinghu, S., Kim, J.H., Jang, J.W., Li, Y.H., Goh, Y.M., Chi, X.Z., et al. (2010). Runx3 is required for the differentiation of lung epithelial cells and suppression of lung cancer. Oncogene *29*, 3349-3361.

Lee, Y.S., Lee, J.W., Jang, J.W., Chi, X.Z., Kim, J.H., Li, Y.H., Kim, M.K., Kim, D.M., Choi, B.S., Kim, E.G., et al. (2013). Runx3 inactivation is a crucial early event in the development of lung adenocarcinoma. Cancer Cell *24*, 603-616.

Muzumdar, M.D., Dorans, K.J., Chung, K.M., Robbins, R., Tammela, T., Gocheva, V., Li, C.M., and Jacks, T. (2016). Clonal dynamics following p53 loss of heterozygosity in Kras-driven cancers. Nat. Commun. *7*, 12685.

Podsypanina, K., Politi, K., Beverly, L.J., and Varmus, H.E. (2008). Oncogene cooperation in tumor maintenance and tumor recurrence in mouse mammary tumors induced by Myc and mutant Kras. Proc. Natl. Acad. Sci. U. S. A. *105*, 5242-5247.

Samarakkody, A.S., Shin, N.Y., and Cantor, A.B. (2020). Role of RUNX family transcription factors in DNA damage response. Mol. Cells *43*, 99-106.

Seo, W. and Taniuchi, I. (2020). The roles of RUNX family proteins in development of immune cells. Mol. Cells *43*, 107-113.

Serrano, M., Lin, A.W., McCurrach, M.E., Beach, D., and Lowe, S.W. (1997). Oncogenic ras provokes premature cell senescence associated with accumulation of p53 and p16INK4a. Cell *88*, 593-602.

Shao, D.D., Xue, W., Krall, E.B., Bhutkar, A., Piccioni, F., Wang, X., Schinzel, A.C., Sood, S., Rosenbluh, J., Kim, J.W., et al. (2014). KRAS and YAP1 converge to regulate EMT and tumor survival. Cell *158*, 171-184.

Subramanian, J. and Govindan, R. (2008). Molecular genetics of lung cancer in people who have never smoked. Lancet Oncol. *9*, 676-682.

Tuveson, D.A., Shaw, A.T., Willis, N.A., Silver, D.P., Jackson, E.L., Chang, S., Mercer, K.L., Grochow, R., Hock, H., Crowley, D., et al. (2004). Endogenous oncogenic K-ras(G12D) stimulates proliferation and widespread neoplastic and developmental defects. Cancer Cell *5*, 375-387.

Weinberg, R.A. (2014). pRb and control of the cell cycle clock. In The Biology of Cancer, R.A. Weinberg, eds. (New York: Garland Science), pp. 275-329.

Westcott, P.M., Halliwill, K.D., To, M.D., Rashid, M., Rust, A.G., Keane, T.M., Delrosario, R., Jen, K.Y., Gurley, K.E., Kemp, C.J., et al. (2015). The mutational landscapes of genetic and chemical models of Kras-driven lung cancer. Nature *517*, 489-492.

Wistuba, I.I. and Gazdar, A.F. (2006). Lung cancer preneoplasia. Annu. Rev. Pathol. *1*, 331-348.

Xue, J.Y., Zhao, Y., Aronowitz, J., Mai, T.T., Vides, A., Qeriqi, B., Kim, D., Li, C., de Stanchina, E., Mazutis, L., et al. (2020). Rapid non-uniform adaptation to conformation-specific KRAS(G12C) inhibition. Nature *577*, 421-425.